Genetic autophagy enhancement improves neuroinflammation and recovery after spinal cord injury via transcriptomic modulation

Zhuofan Lei, Yun Li, Hui Li, Junfang Wu*

Department of Anesthesiology and Center for Shock, Trauma and Anesthesiology Research (STAR), University of Maryland School of Medicine, Baltimore, MD 21201, USA.

*Corresponding authors

Junfang Wu, email: Junfang.Wu@som.umaryland.edu, phone: 410-706-5189

Supplementary Information

Supplemental Information comprises nine supplemental figures with corresponding legends and two supplemental tables.

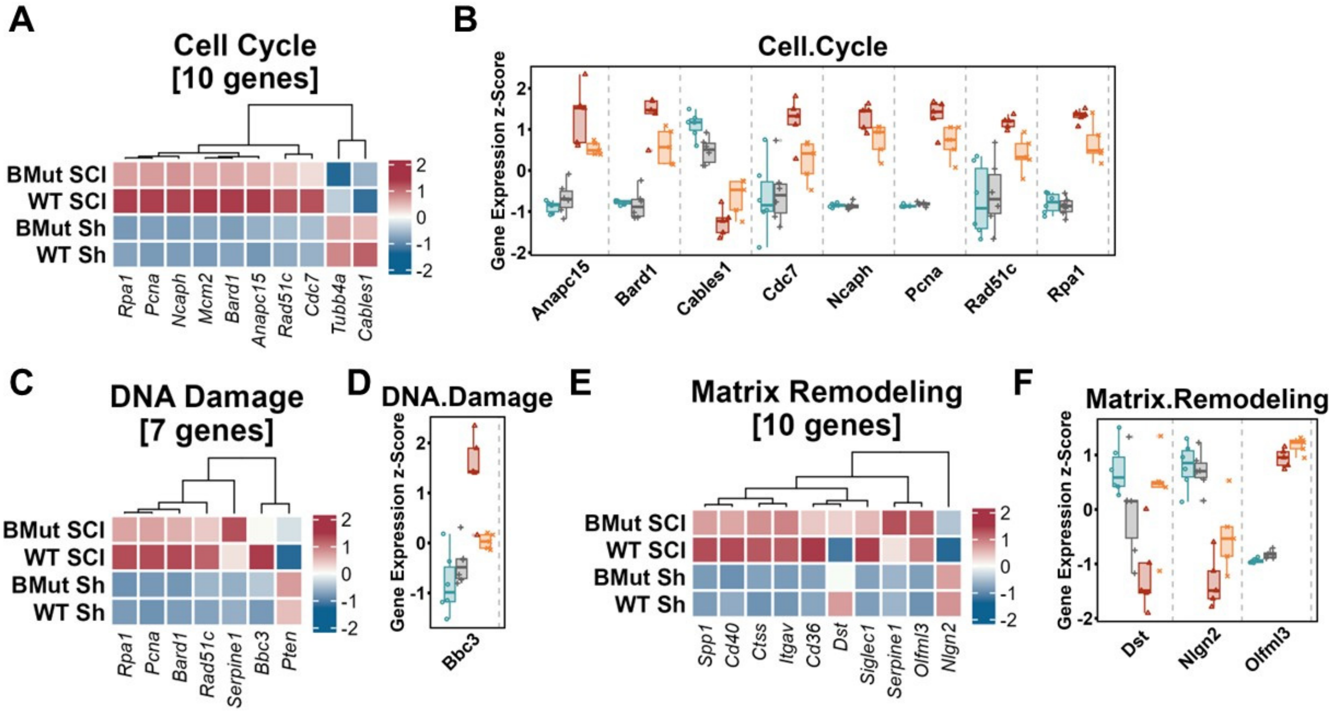

Supplementary Figure 1. Genetic enhancement of autophagy in Becn1$^{F121A/F121A}$ mice (BMut) shows different gene responses in pathways of Cell Cycle, DNA damage, and Matrix Remodeling in inured spinal cord tissues (SPC) at 3 days post-injury. (A) A heatmap of gene z-scores involved in Cell Cycle pathway based on the differential expressed genes (DEGs) from Fig.1C. **(B)** Box plots of the representative genes among the four groups included in (A). **(C-F)** Heatmaps and box plots were displayed for pathways of DNA damage (C-D) and Matrix Remodeling (E-F). n=6 mice (Sham) and 5 mice (SCI) each group.

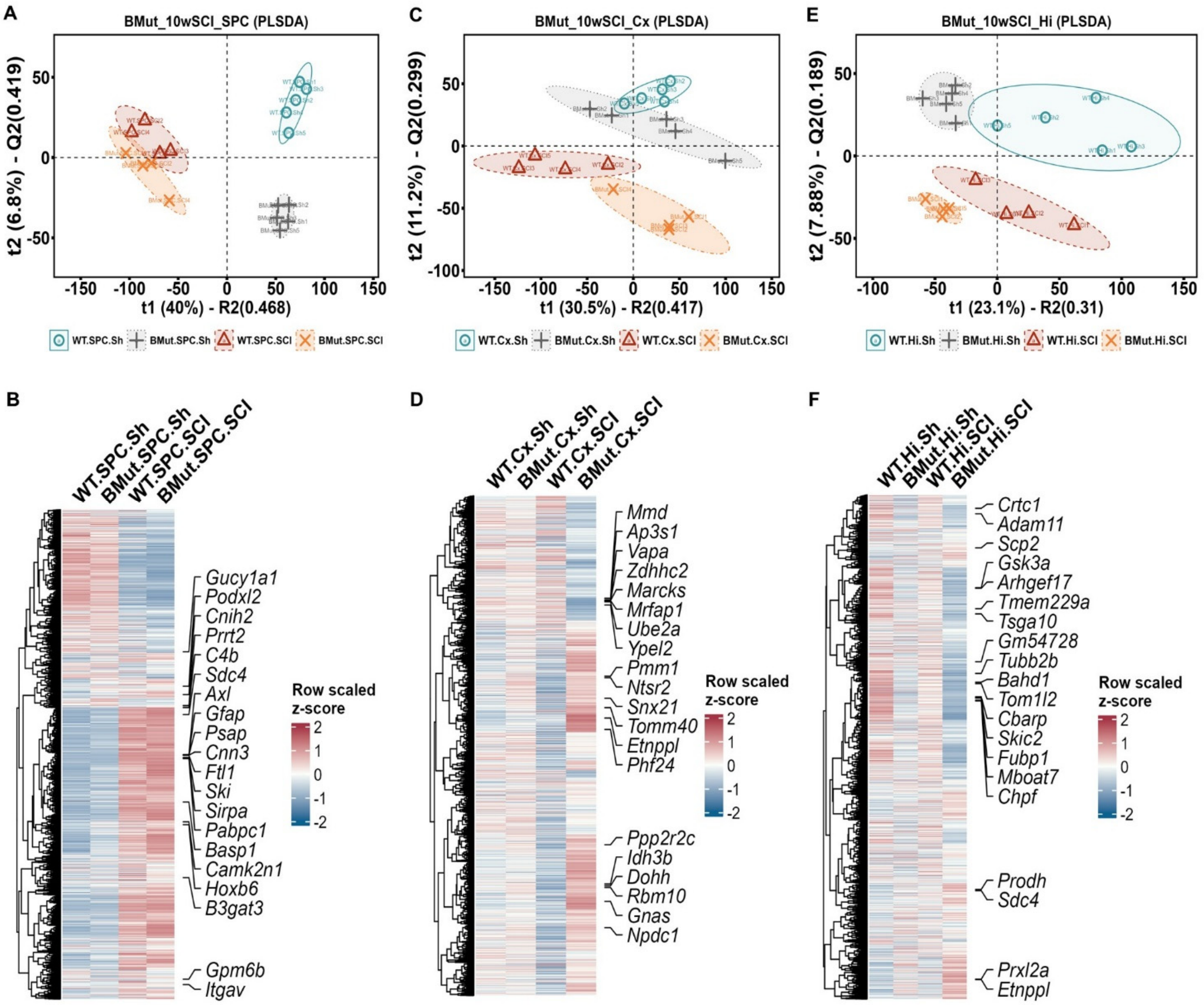

Supplementary Figure 2. Comparative transcriptomic profiling of spinal cord tissues (SPC), somatosensory cortex (Cx), and hippocampus (Hi) between Becn1$^{F121A/F121A}$ (BMut) and WT mice at 10 weeks after SCI. (A) Partial Least Squares Discriminant Analysis (PLS-DA) plot of the raw RNA-seq data from SPC indicated that the two main principal components of variation were captured on the x- and y-axis, respectively, showing a clear separation of clusters between the Sham (Sh) and SCI groups. **(B)** Gene expression profiles from SPC RNA-seq were visualized as z-score heatmaps, with top 20 genes marked based on PLS-DA. **(C-F)** The PLS-DA plots and heatmaps of the RNAseq data were shown for Cx (C-D) and Hi (E-F). n=5 mice (Sham) and 4 mice (SCI) each group.

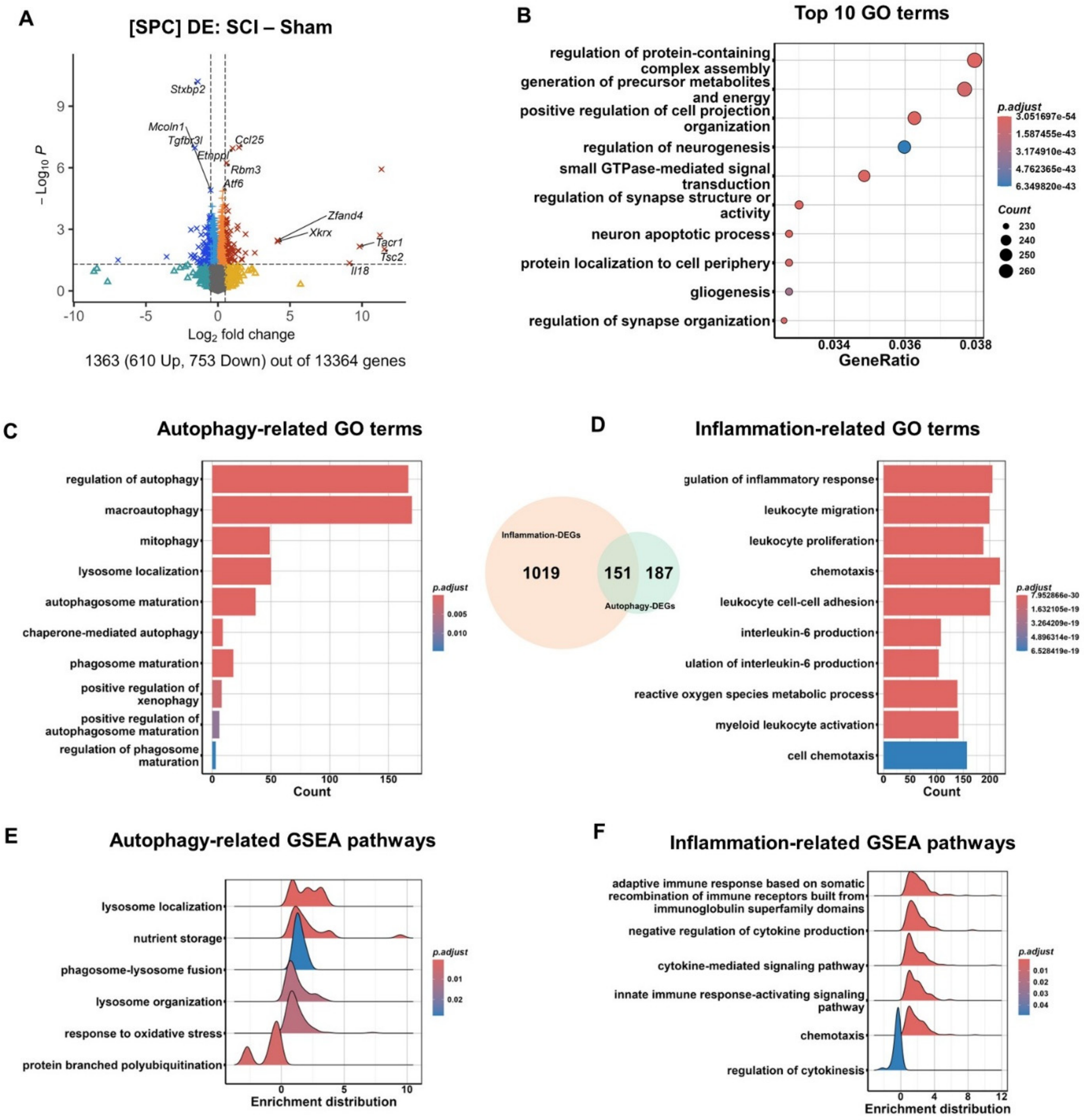

Supplementary Figure 3. Chronic SCI potentiates the immune response and activated autophagy-lysosome pathways in spinal cord tissue (SPC) of both Becn1$^{F121A/F121A}$ and WT mice. (A) The volcano plot displayed the significance and fold changes of all genes from the differential expression analysis comparing the injury effect in SPC of SCI versus Sham. **(B)** Top 10 enriched GO terms derived from DEGs showing a significant injury effect in (A). **(C)** Top 10 GO terms related to Autophagy process. **(D)** Top 10 GO terms related to inflammation and immune responses. **(E)** GSEA terms indicating dysregulation of autophagy-related signaling pathways. **(F)** Neuroinflammation-related functional pathways that were upregulated or downregulated according to GSEA.

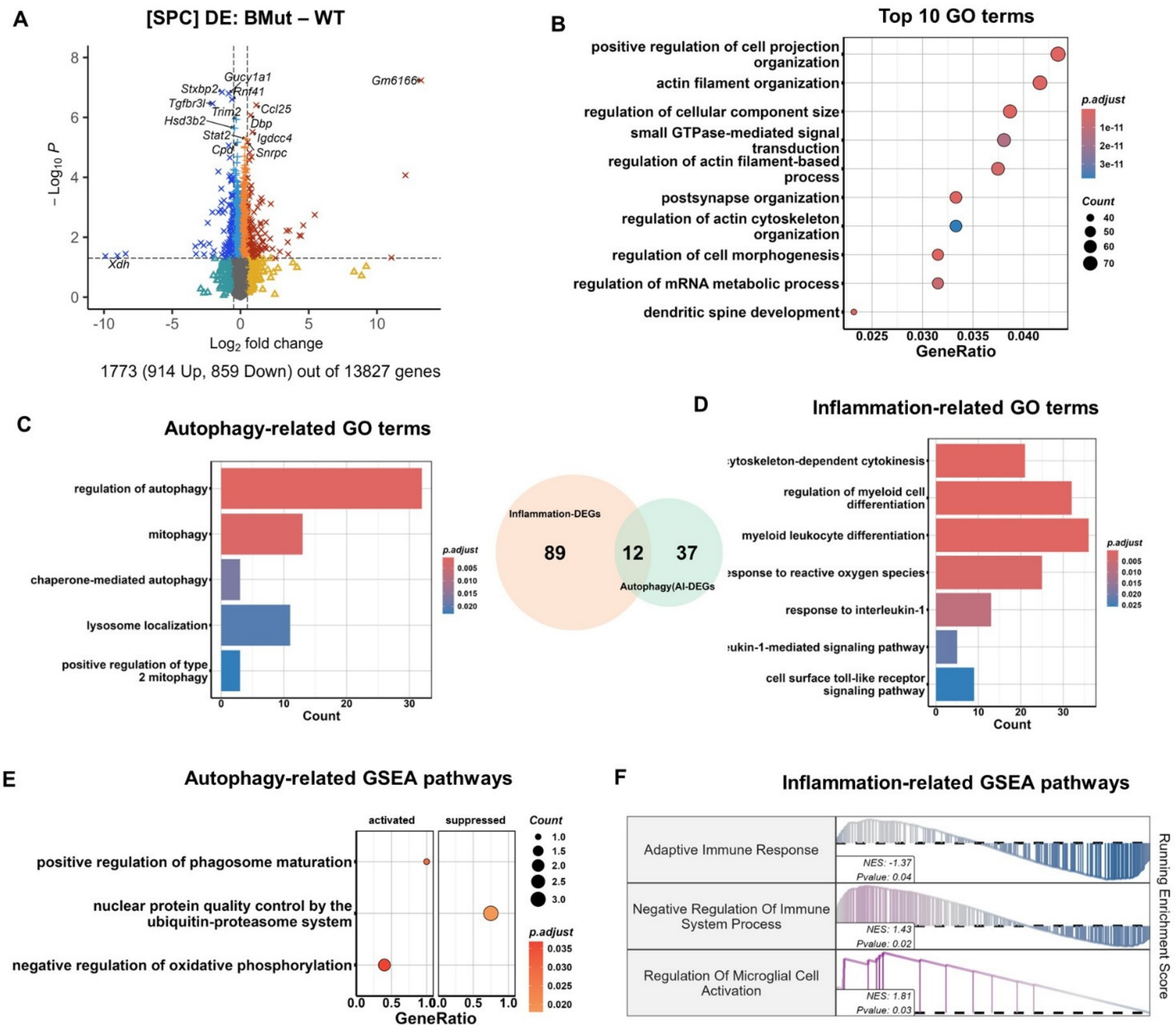

Supplementary Figure 4. Becn1$^{F121A/F121A}$ mutation (BMut) alters the expression of genes involved in autophagy- and inflammation-related pathways in spinal cord tissue (SPC) 10 weeks after SCI. (A) The volcano plot displays the significance and fold changes of all genes from the differential expression analysis of the genotype effect in SPC, comparing BMut to WT. **(B)** Top 10 enriched GO terms derived from DEGs with significant genotype effect in (A). **(C)** Top GO terms related to Autophagy process. **(D)** Top GO terms related to inflammation and immune responses. **(E)** GSEA terms indicating the activation or suppression of Autophagy related signaling pathways. **(F)** Functionally activated or suppressed neuroinflammatory pathways identified by GSEA.

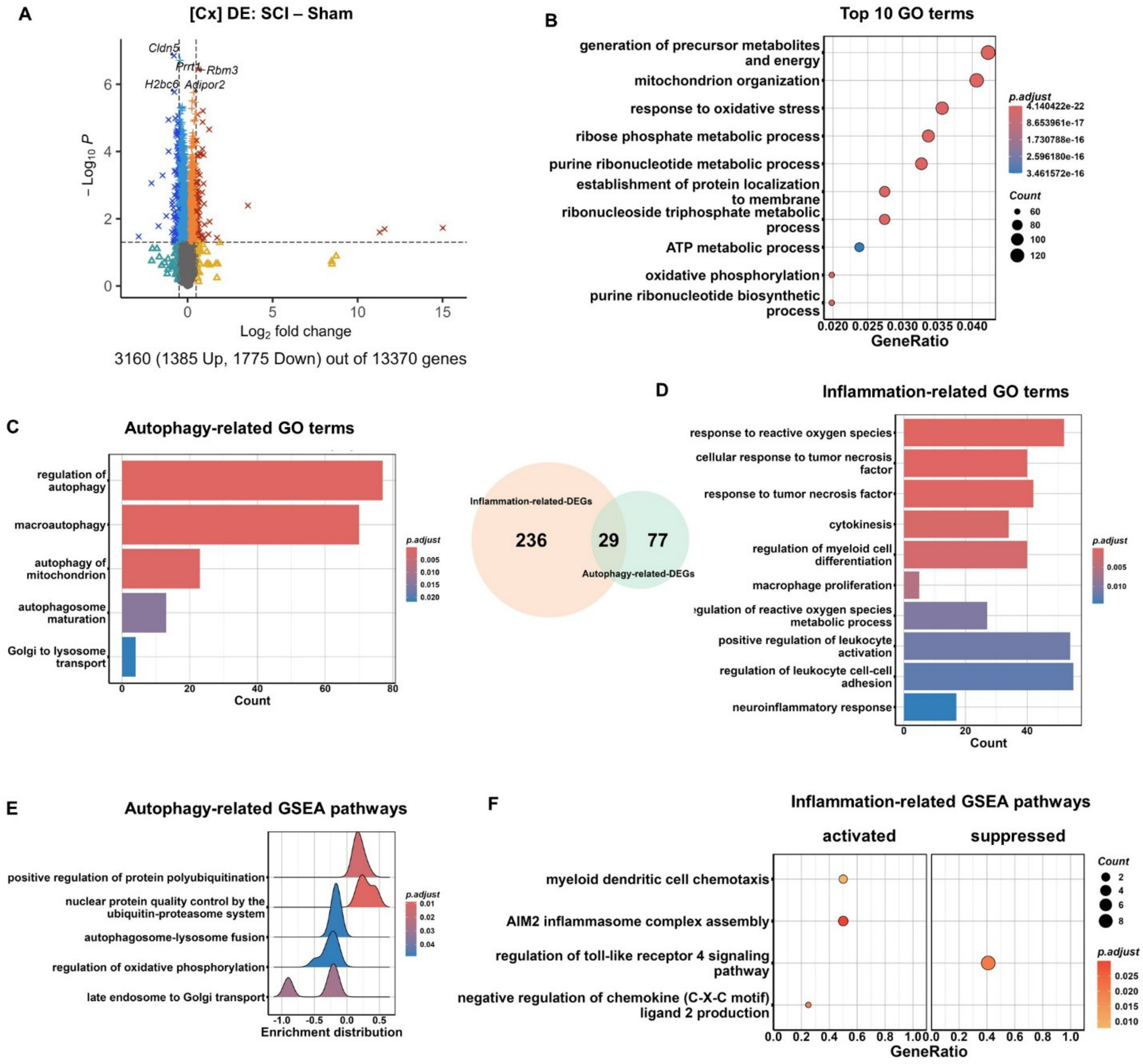

Supplementary Figure 5. SCI impairs autophagy-lysosome pathways with inflammatory homeostasis perturbed in somatosensory cortex (Cx) 10 weeks after SCI. (A) The volcano plot displayed the significance and fold changes of all genes from the differential expression genes (DEGs) analysis of injury effects in the Cx (SCI vs. Sham). **(B)** Top 10 enriched GO terms derived from DEGs with significant injury effect in (A). **(C)** Top 10 GO terms related to Autophagy process. **(D)** Top 10 GO terms related to inflammation and immune responses. **(E)** Gene Set Enrichment Analysis (GSEA) terms indicating the dysregulation of Autophagy related signaling pathways. **(F)** Neuroinflammation-related pathways found to be up- or down-regulated based on GSEA.

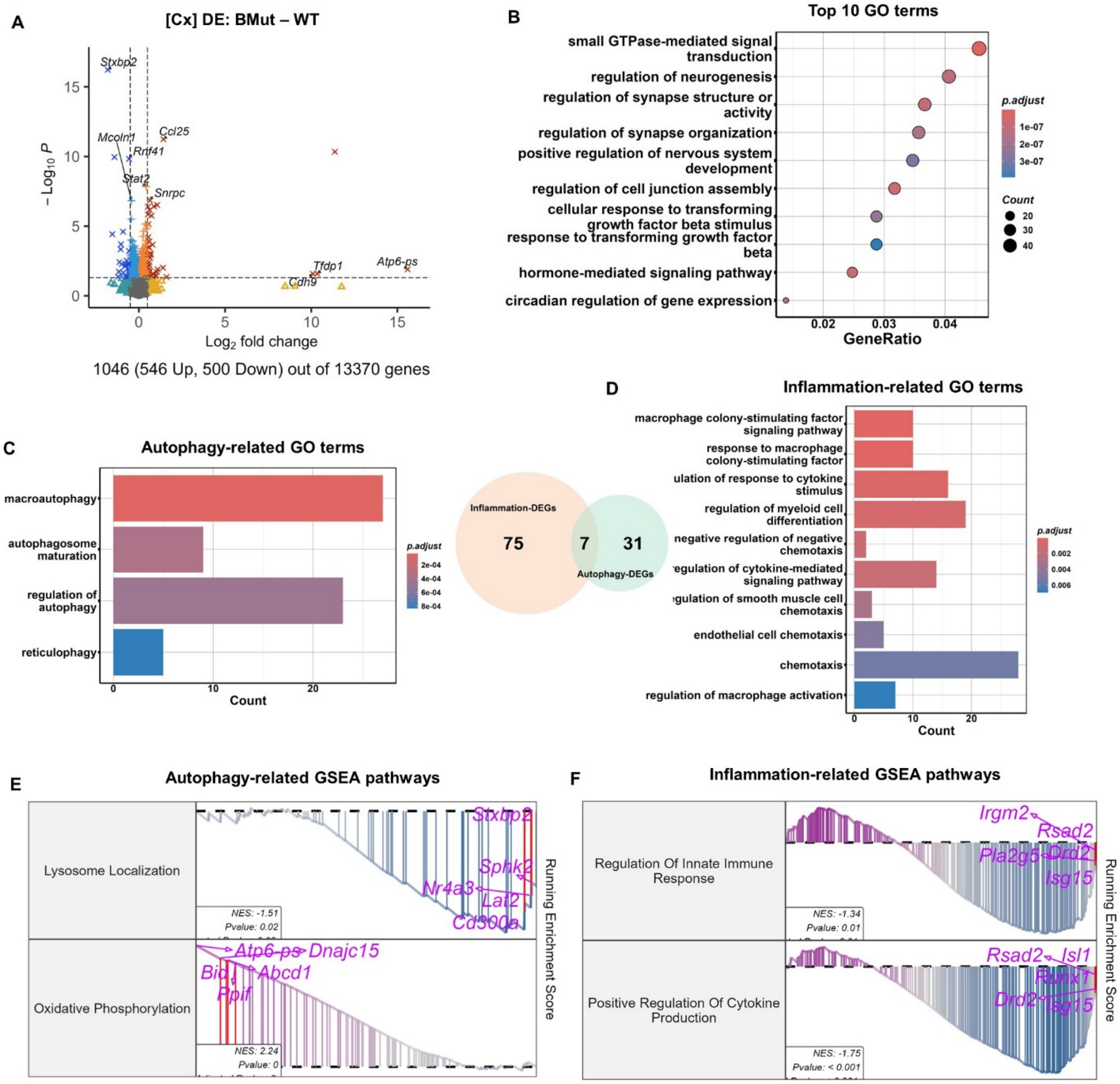

Supplementary Figure 6. Becn1$^{F121A/F121A}$ mutation mitigates immune responses by regulating autophagy-lysosome pathways in somatosensory cortex (Cx). (A) The volcano plot displays the significance and fold changes of all genes from the differential expression genes (DEGs) analysis of genotype effects in the Cx (BMut vs. WT). **(B)** Top 10 enriched GO terms derived from DEGs with significant injury effect in (A). **(C)** Top GO terms related to Autophagy process. **(D)** Top GO terms related to inflammation and immune responses. **(E)** Gene Set Enrichment Analysis (GSEA) revealed suppression of the 'Lysosome Localization' pathway and activation of the 'Oxidative Phosphorylation' pathway, both related to autophagy. **(F)** GSEA identified terms associated with the suppression of neuroinflammation-related signaling pathways.

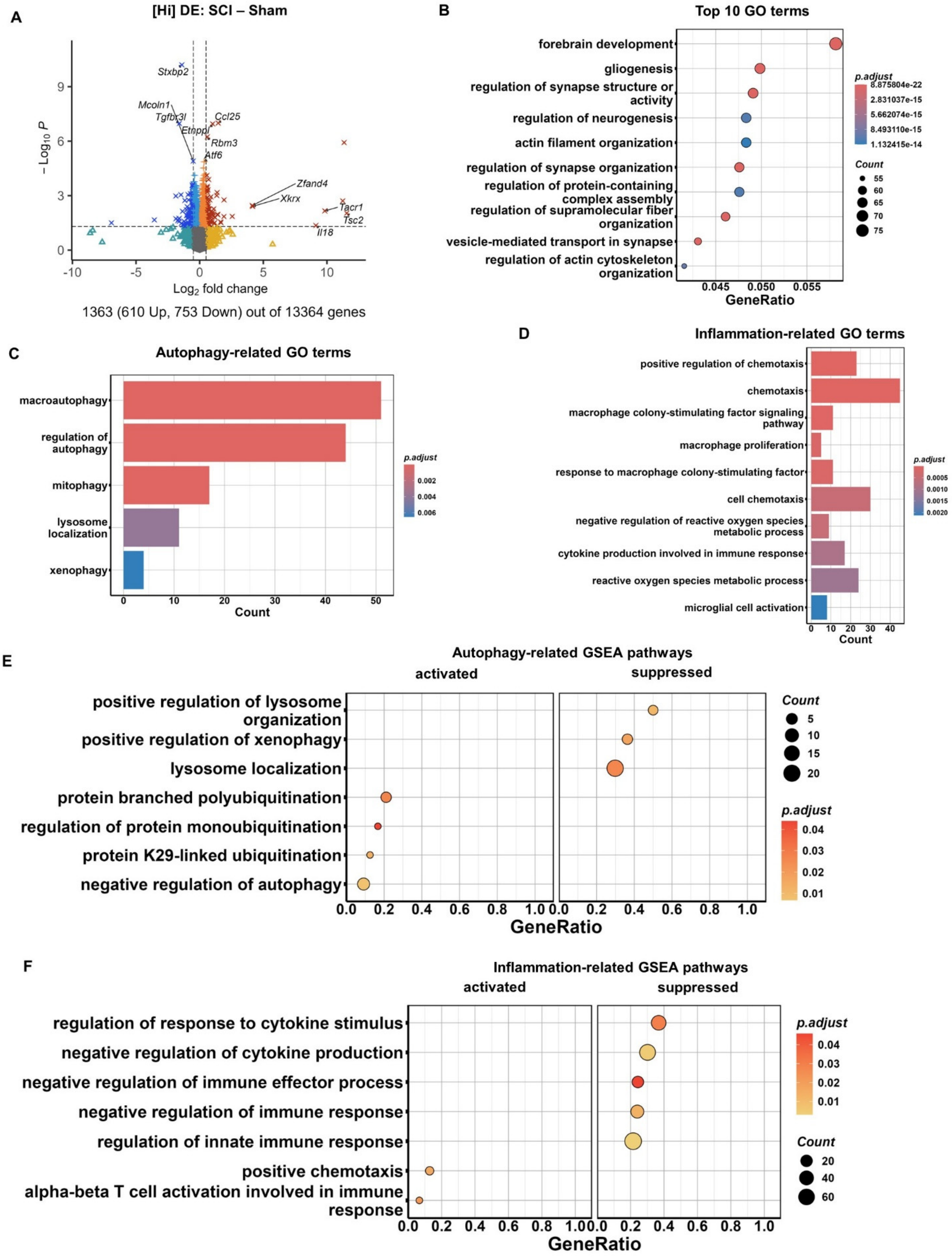
A
[Hi] DE: SCI – Sham
$-\mathrm{Log}_{10}\,P$
0
3
6
9
Stxbp2
Mcoln1
Tgfbr3l
Etnppl
Ccl25
Rbm3
Atf6
Zfand4
Xkrx
Tacr1
Tsc2
Il18
-10
-5
0
5
10
Log_2 fold change
1363 (610 Up, 753 Down) out of 13364 genes
B
Top 10 GO terms
forebrain development
gliogenesis
regulation of synapse structure or activity
regulation of neurogenesis
actin filament organization
regulation of synapse organization
regulation of protein-containing complex assembly
regulation of supramolecular fiber organization
vesicle-mediated transport in synapse
regulation of actin cytoskeleton organization
0.045
0.050
0.055
GeneRatio
p.adjust
8.875804e-22
2.831037e-15
5.662074e-15
8.493110e-15
1.132415e-14
Count
55
60
65
70
75
C
Autophagy-related GO terms
macroautophagy
regulation of autophagy
mitophagy
lysosome localization
xenophagy
0
10
20
30
40
50
Count
p.adjust
0.002
0.004
0.006
D
Inflammation-related GO terms
positive regulation of chemotaxis
chemotaxis
macrophage colony-stimulating factor signaling pathway
macrophage proliferation
response to macrophage colony-stimulating factor
cell chemotaxis
negative regulation of reactive oxygen species metabolic process
cytokine production involved in immune response
reactive oxygen species metabolic process
microglial cell activation
0
10
20
30
40
Count
p.adjust
0.0005
0.0010
0.0015
0.0020
E
Autophagy-related GSEA pathways
activated
suppressed
positive regulation of lysosome organization
positive regulation of xenophagy
lysosome localization
protein branched polyubiquitination
regulation of protein monoubiquitination
protein K29-linked ubiquitination
negative regulation of autophagy
0.0
0.2
0.4
0.6
0.8
1.0
GeneRatio
Count
5
10
15
20
p.adjust
0.04
0.03
0.02
0.01
F
Inflammation-related GSEA pathways
activated
suppressed
regulation of response to cytokine stimulus
negative regulation of cytokine production
negative regulation of immune effector process
negative regulation of immune response
regulation of innate immune response
positive chemotaxis
alpha-beta T cell activation involved in immune response
0.0
0.2
0.4
0.6
0.8
1.0
GeneRatio
p.adjust
0.04
0.03
0.02
0.01
Count
20
40
60

Supplementary Figure 7. SCI dysregulates Autophagy-lysosome signaling and immune responses in mouse hippocampus 10 weeks post-injury. (A) The volcano plot displays the significance and fold changes of all genes from the differential expression genes (DEGs) analysis of injury effects in the hippocampus (SCI vs. Sham). **(B)** Top 10 enriched GO terms derived from DEGs with significant injury effect in (A). **(C)** Top GO terms related to Autophagy process. **(D)** Top 10 GO terms related to inflammation and immune responses. **(E-F)** GSEA terms showing activation or suppression of autophagy-related signaling pathways (E) and neuroinflammation-related functional pathways (F).

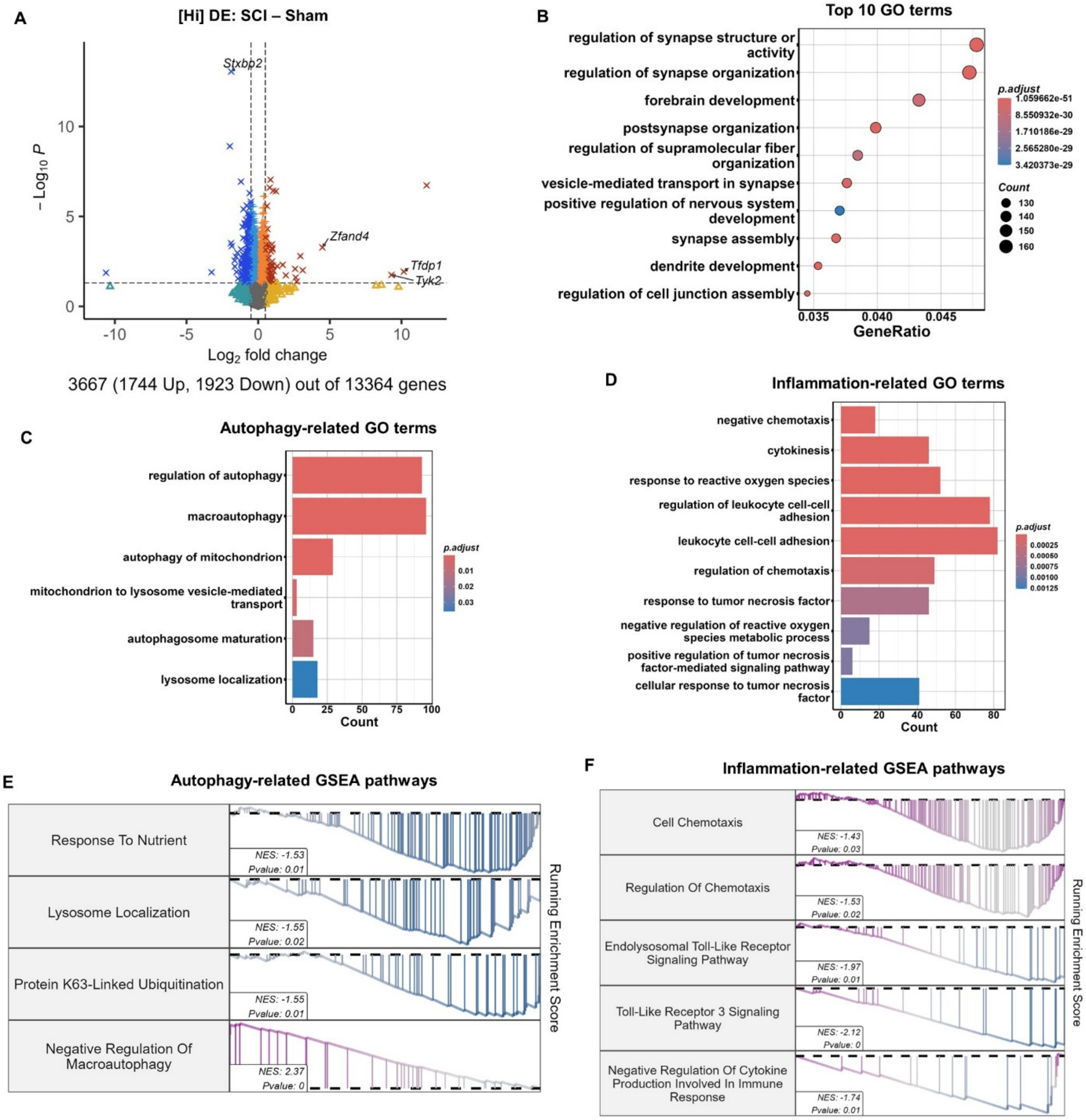

Supplementary Figure 8. Becn1$^{F121A/F121A}$ mutation (BMut) regulates autophagy-lysosome pathways accompanied by alleviated proinflammatory responses in the hippocampus (Hi). **(A)** The volcano plot shows the significance and fold changes of all genes from the differential expression genes (DEGs) analysis of genotype effects in the hippocampus (BMut vs. WT). **(B)** Top 10 enriched GO terms derived from DEGs with significant injury effect in (A). **(C)** Top GO terms related to Autophagy process. **(D)** Top GO terms related to inflammation and immune responses. **(E-F)** GSEA terms showing conversely regulation of multiple Autophagy-related signaling pathways (E) and suppressed functional pathway of “Cell Chemotaxis” and “Regulation of Chemotaxis” (F).

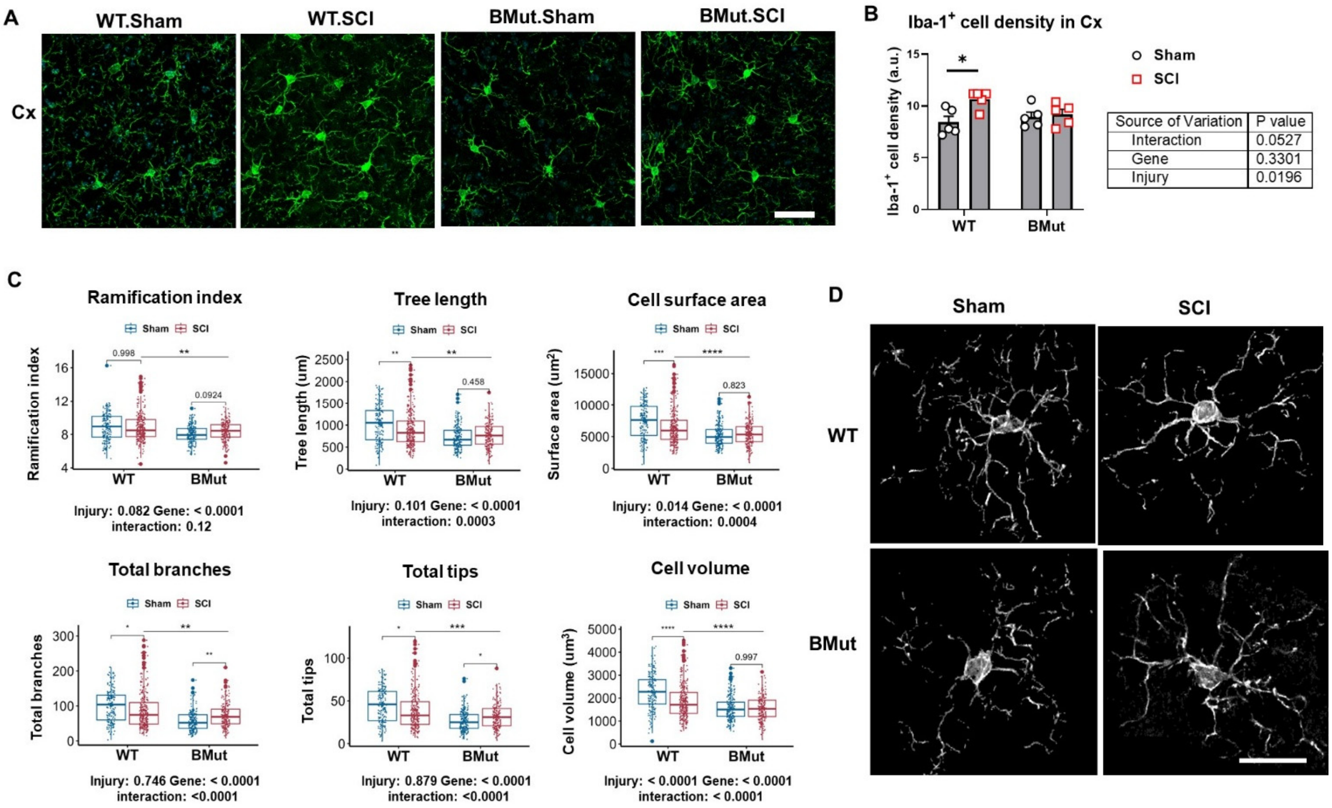

Supplementary Figure 9. Becn1$^{F121A/F121A}$ mutation (BMut) altes microglial responses to SCI in somatosensory cortex (Cx). (A) Representative confocal images showed microglia stained by Iba-1 with DAPI in mice Cx. **(B)** Microglial cell numbers were quantified per field of view under 100x magnification. n=5 mice/group. **(C)** Typical morphological characteristics revealed the different response to SCI in microglia cells in Cx of BMut mice compared to WT. N=170 cells from 5 WT.Sham mice; N=196 cells from 5 Bmut.Sham mice; N=262 cells from 5 WT.SCI mice; N=178 cells from 5 BMut.SCI mice. **(D)** Representative images of Cx microglia cells after MotiQ processing. Scale bars=20 μm (A) and 50 μm (D). *p<0.05; **p<0.01; ***p<0.001; ****p<0.0001; Two-way ANOVA with Turkey's test for (B-C).

Supplemental Table 1. Becn1$^{F121A/F121A}$ mutation (BMut) modulates pathway enrichment scores of the NanoString Neuroinflammation Panel in acutely injured spinal cord tissue (SPC).

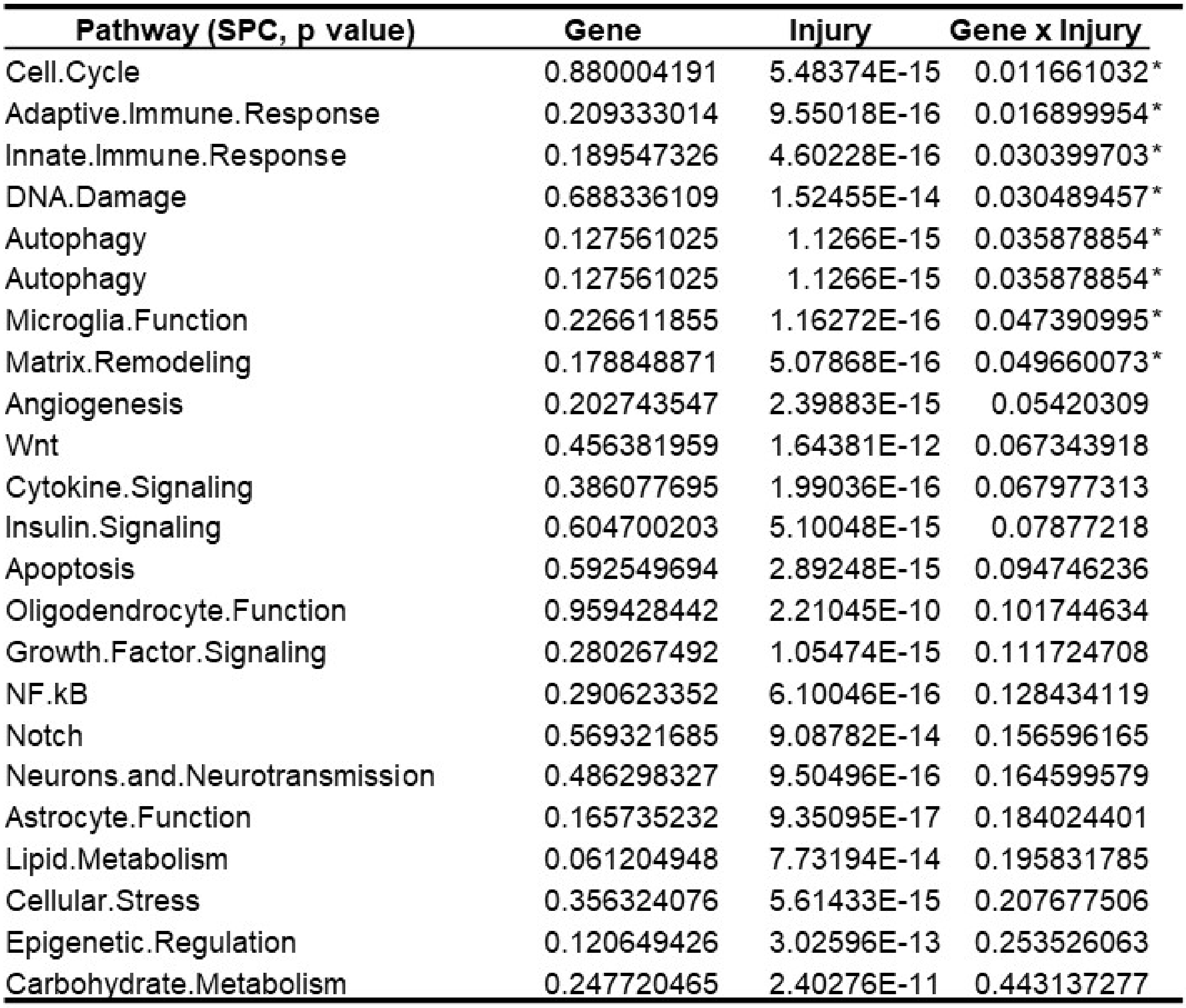

Pathway (SPC, p value)	Gene	Injury	Gene x Injury
Cell.Cycle	0.880004191	5.48374E-15	0.011661032*
Adaptive.Immune.Response	0.209333014	9.55018E-16	0.016899954*
Innate.Immune.Response	0.189547326	4.60228E-16	0.030399703*
DNA.Damage	0.688336109	1.52455E-14	0.030489457*
Autophagy	0.127561025	1.1266E-15	0.035878854*
Autophagy	0.127561025	1.1266E-15	0.035878854*
Microglia.Function	0.226611855	1.16272E-16	0.047390995*
Matrix.Remodeling	0.178848871	5.07868E-16	0.049660073*
Angiogenesis	0.202743547	2.39883E-15	0.05420309
Wnt	0.456381959	1.64381E-12	0.067343918
Cytokine.Signaling	0.386077695	1.99036E-16	0.067977313
Insulin.Signaling	0.604700203	5.10048E-15	0.07877218
Apoptosis	0.592549694	2.89248E-15	0.094746236
Oligodendrocyte.Function	0.959428442	2.21045E-10	0.101744634
Growth.Factor.Signaling	0.280267492	1.05474E-15	0.111724708
NF.kB	0.290623352	6.10046E-16	0.128434119
Notch	0.569321685	9.08782E-14	0.156596165
Neurons.and.Neurotransmission	0.486298327	9.50496E-16	0.164599579
Astrocyte.Function	0.165735232	9.35095E-17	0.184024401
Lipid.Metabolism	0.061204948	7.73194E-14	0.195831785
Cellular.Stress	0.356324076	5.61433E-15	0.207677506
Epigenetic.Regulation	0.120649426	3.02596E-13	0.253526063
Carbohydrate.Metabolism	0.247720465	2.40276E-11	0.443137277

P values corresponding to genotype, injury, and their interaction were determined for each pathway using two-way ANOVA. n=6 mice (Sham) and 5 mice (SCI) each group.

Supplemental Table 2. Becn1$^{F121A/F121A}$ mutation (BMut) alters the gene enrichment scores in the pathways of "Autophagy", "Inflammatory Signaling", "Microglia Function", "Adaptive Immune Response", "Innate Immune Response", "Cell Cycle", "DNA Damage", and "Matrix Remodeling". Spinal cord tissues were harvested at 3 days after SCI and analyzed by the Nanostring Neuroinflammation panel.

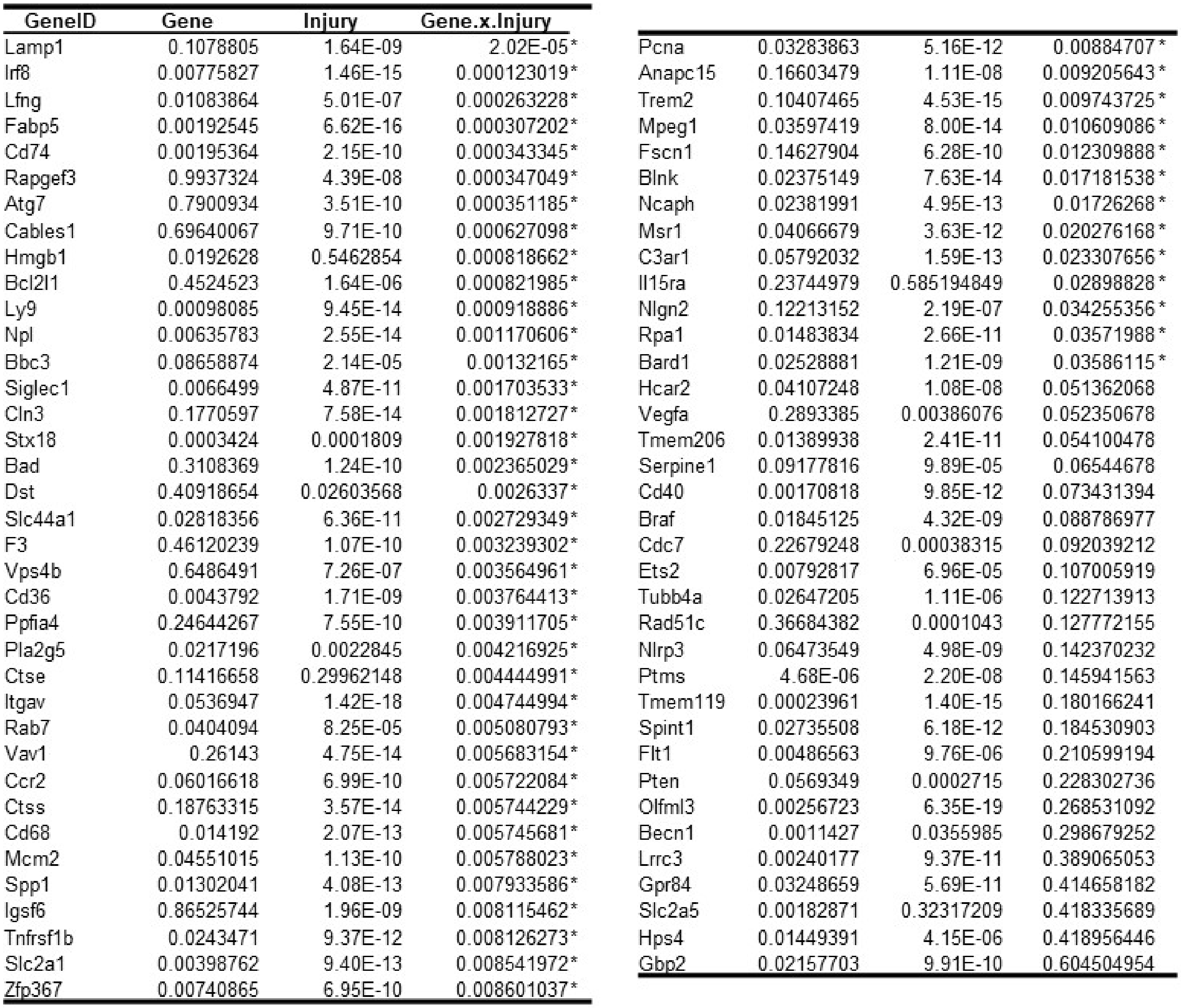

GeneID	Gene	Injury	Gene.x.Injury
Lamp1	0.1078805	1.64E-09	2.02E-05*
Irf8	0.00775827	1.46E-15	0.000123019*
Lfng	0.01083864	5.01E-07	0.000263228*
Fabp5	0.00192545	6.62E-16	0.000307202*
Cd74	0.00195364	2.15E-10	0.000343345*
Rapgef3	0.9937324	4.39E-08	0.000347049*
Atg7	0.7900934	3.51E-10	0.000351185*
Cables1	0.69640067	9.71E-10	0.000627098*
Hmgb1	0.0192628	0.5462854	0.000818662*
Bcl2l1	0.4524523	1.64E-06	0.000821985*
Ly9	0.00098085	9.45E-14	0.000918886*
Npl	0.00635783	2.55E-14	0.001170606*
Bbc3	0.08658874	2.14E-05	0.00132165*
Siglec1	0.0066499	4.87E-11	0.001703533*
Cln3	0.1770597	7.58E-14	0.001812727*
Stx18	0.0003424	0.0001809	0.001927818*
Bad	0.3108369	1.24E-10	0.002365029*
Dst	0.40918654	0.02603568	0.0026337*
Slc44a1	0.02818356	6.36E-11	0.002729349*
F3	0.46120239	1.07E-10	0.003239302*
Vps4b	0.6486491	7.26E-07	0.003564961*
Cd36	0.0043792	1.71E-09	0.003764413*
Ppfia4	0.24644267	7.55E-10	0.003911705*
Pla2g5	0.0217196	0.0022845	0.004216925*
Ctse	0.11416658	0.29962148	0.004444991*
Itgav	0.0536947	1.42E-18	0.004744994*
Rab7	0.0404094	8.25E-05	0.005080793*
Vav1	0.26143	4.75E-14	0.005683154*
Ccr2	0.06016618	6.99E-10	0.005722084*
Ctss	0.18763315	3.57E-14	0.005744229*
Cd68	0.014192	2.07E-13	0.005745681*
Mcm2	0.04551015	1.13E-10	0.005788023*
Spp1	0.01302041	4.08E-13	0.007933586*
Igsf6	0.86525744	1.96E-09	0.008115462*
Tnfrsf1b	0.0243471	9.37E-12	0.008126273*
Slc2a1	0.00398762	9.40E-13	0.008541972*
Zfp367	0.00740865	6.95E-10	0.008601037*
Pcna	0.03283863	5.16E-12	0.00884707*
Anapc15	0.16603479	1.11E-08	0.009205643*
Trem2	0.10407465	4.53E-15	0.009743725*
Mpeg1	0.03597419	8.00E-14	0.010609086*
Fscn1	0.14627904	6.28E-10	0.012309888*
Blnk	0.02375149	7.63E-14	0.017181538*
Ncaph	0.02381991	4.95E-13	0.01726268*
Msr1	0.04066679	3.63E-12	0.020276168*
C3ar1	0.05792032	1.59E-13	0.023307656*
Il15ra	0.23744979	0.585194849	0.02898828*
Nlgn2	0.12213152	2.19E-07	0.034255356*
Rpa1	0.01483834	2.66E-11	0.03571988*
Bard1	0.02528881	1.21E-09	0.03586115*
Hcar2	0.04107248	1.08E-08	0.051362068
Vegfa	0.2893385	0.00386076	0.052350678
Tmem206	0.01389938	2.41E-11	0.054100478
Serpine1	0.09177816	9.89E-05	0.06544678
Cd40	0.00170818	9.85E-12	0.073431394
Braf	0.01845125	4.32E-09	0.088786977
Cdc7	0.22679248	0.00038315	0.092039212
Ets2	0.00792817	6.96E-05	0.107005919
Tubb4a	0.02647205	1.11E-06	0.122713913
Rad51c	0.36684382	0.0001043	0.127772155
Nlrp3	0.06473549	4.98E-09	0.142370232
Ptms	4.68E-06	2.20E-08	0.145941563
Tmem119	0.00023961	1.40E-15	0.180166241
Spint1	0.02735508	6.18E-12	0.184530903
Flt1	0.00486563	9.76E-06	0.210599194
Pten	0.0569349	0.0002715	0.228302736
Olfml3	0.00256723	6.35E-19	0.268531092
Becn1	0.0011427	0.0355985	0.298679252
Lrrc3	0.00240177	9.37E-11	0.389065053
Gpr84	0.03248659	5.69E-11	0.414658182
Slc2a5	0.00182871	0.32317209	0.418335689
Hps4	0.01449391	4.15E-06	0.418956446
Gbp2	0.02157703	9.91E-10	0.604504954

P values corresponding to genotype, injury, and their interaction were determined for each pathway using two-way ANOVA. n=6 mice (Sham) and 5 mice (SCI) each group.